Supplement of Hydrol. Earth Syst. Sci., 28, 1383–1401, 2024
https://doi.org/10.5194/hess-28-1383-2024-supplement

Hydrology and Earth System Sciences
Open Access
EGU

Supplement of

Potential for historically unprecedented Australian droughts from natural variability and climate change

Georgina M. Falster et al.

Correspondence to: Georgina M. Falster (georgina.falster@anu.edu.au)

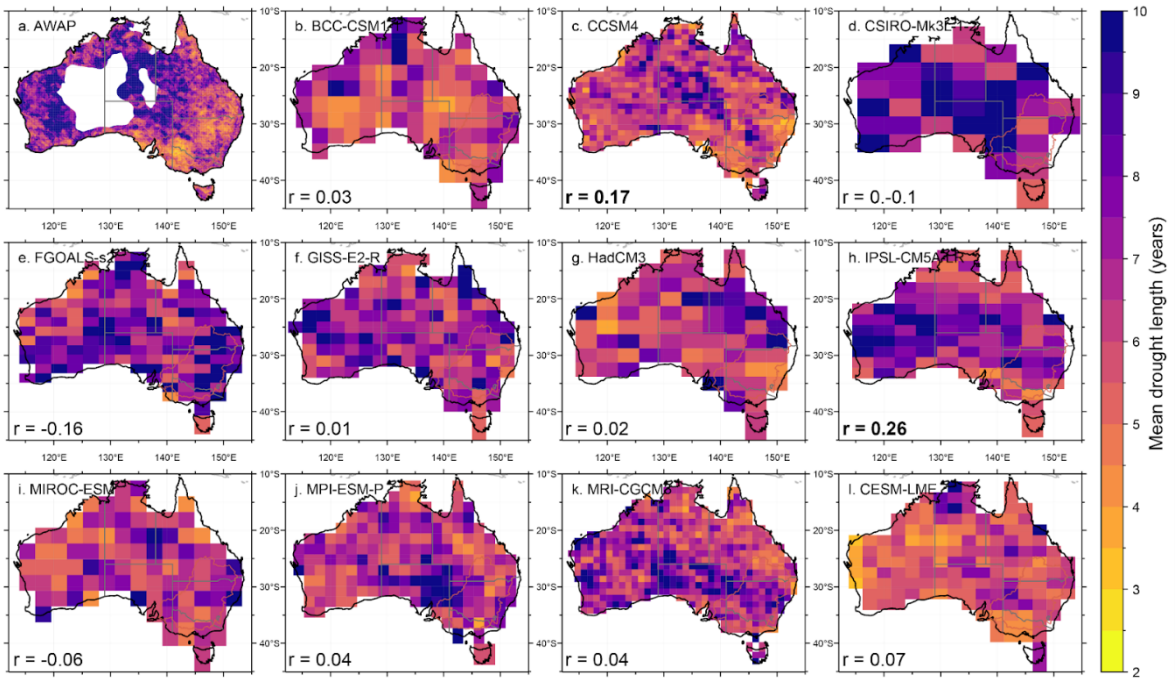

Figure S1: Mean multi-year drought length in (a) observations (1900-2000) and (b-l) model simulations of the same period. Panel (l) shows the CESM-LME ensemble mean. Spatial correlations of each model with observations are shown in the lower left corner in b–l. Bold text denotes a significant ($p < 0.05$) correlation.

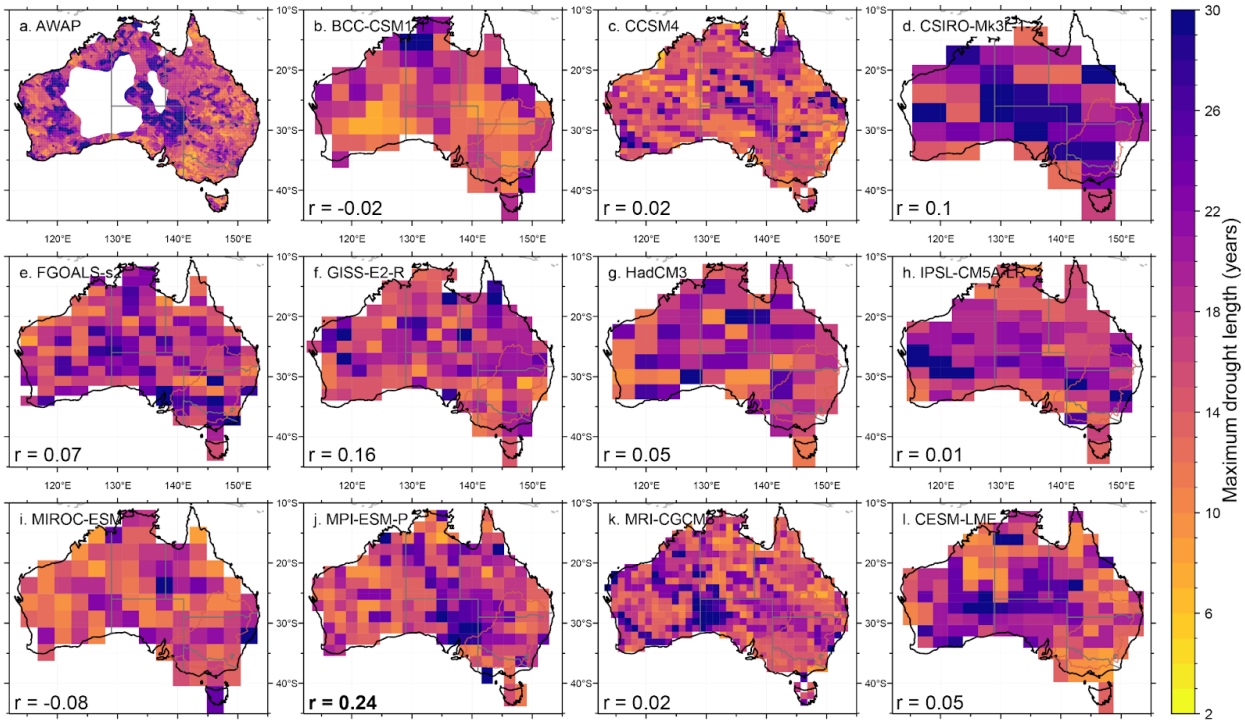

Figure S2: Maximum multi-year drought length in (a) observations (1900-2000) and (b-l) model simulations of the same period. Panel (l) shows the CESM-LME ensemble mean. Spatial correlations of each model with observations are shown in the lower left corner in b–l. Bold text denotes a significant ($p < 0.05$) correlation.

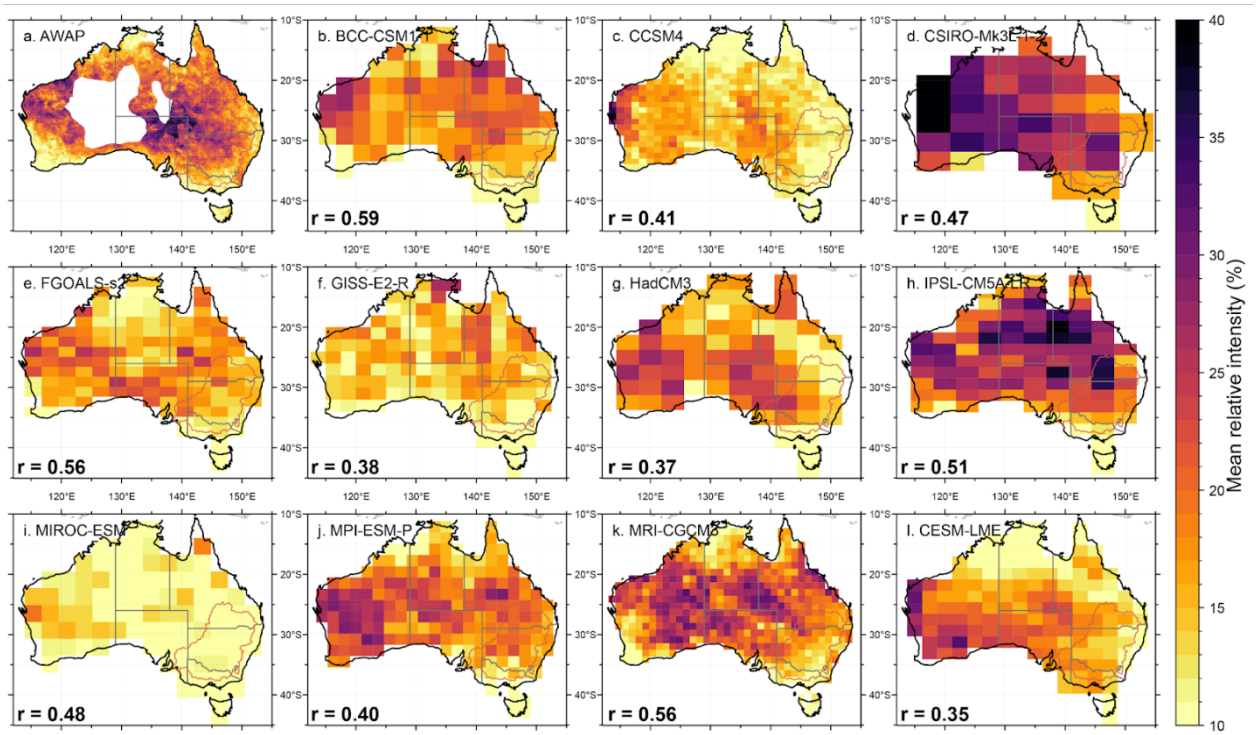

Figure S3: Relative intensity of multi-year droughts in (a) observations (1900–2000) and (b–l) model simulations of the same period. Panel (l) shows the CESM-LME ensemble mean. Spatial correlations of each model with observations are shown in the lower left corner in b–l. Bold text denotes a significant ($p < 0.05$) correlation.

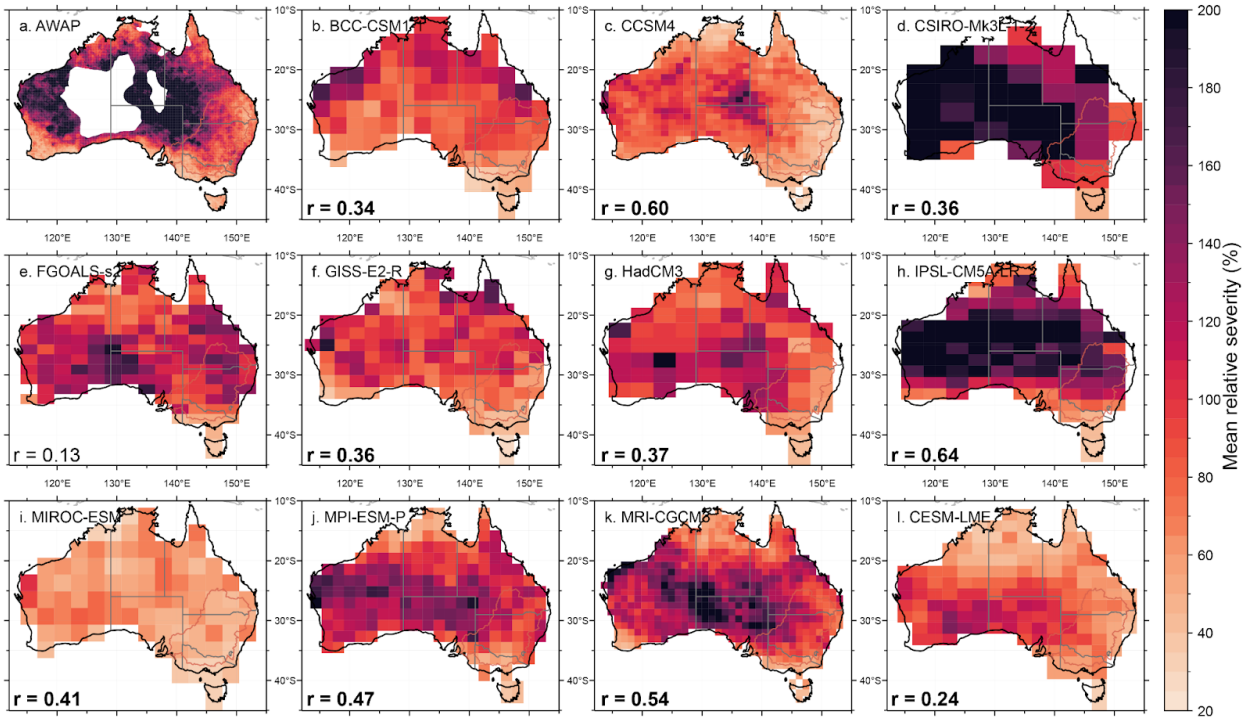

Figure S4: Relative severity of multi-year droughts in (a) observations (1900–2000) and (b–l) model simulations of the same period. Panel (l) shows the CESM-LME ensemble mean. Spatial correlations of each model with observations are shown in the lower left corner in b–l. Bold text denotes a significant ($p < 0.05$) correlation.

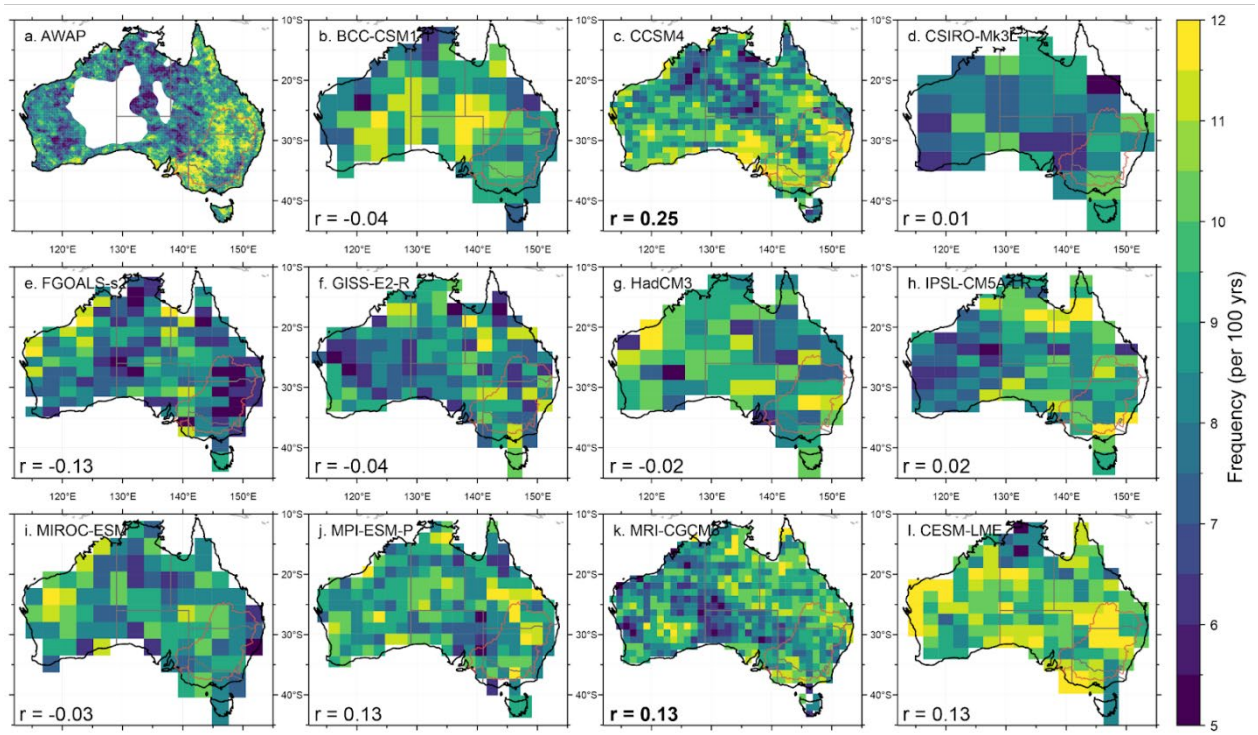

Figure S5: Frequency of multi-year droughts (per 100 years) in (a) observations (1900–2000) and (b–l) model simulations of the same period. Panel (l) shows the CESM-LME ensemble mean. Spatial correlations of each model with observations are shown in the lower left corner in b–l. Bold text denotes a significant ($p < 0.05$) correlation.

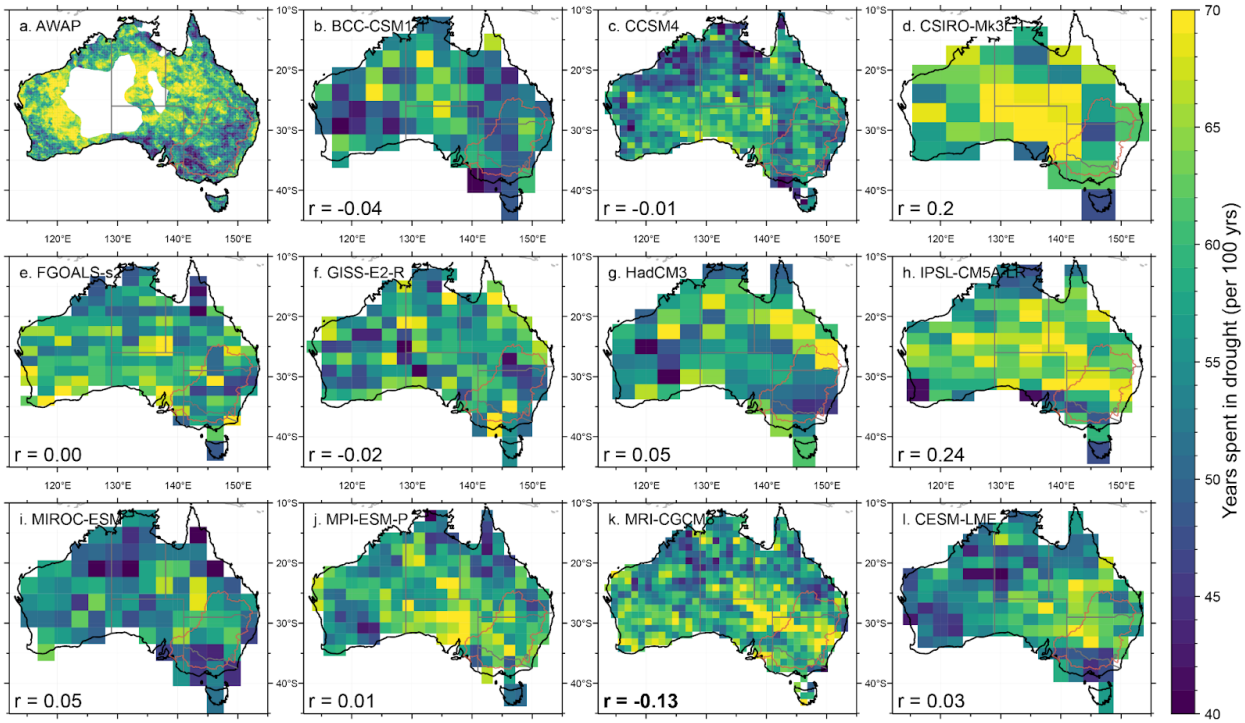

Figure S6: Total years spent in drought (per 100 years) in (a) observations (1900–2000) and (b–l) model simulations of the same period. Panel (l) shows the CESM-LME ensemble mean. Spatial correlations of each model with observations are shown in the lower left corner in b–l. Bold text denotes a significant ($p < 0.05$) correlation.

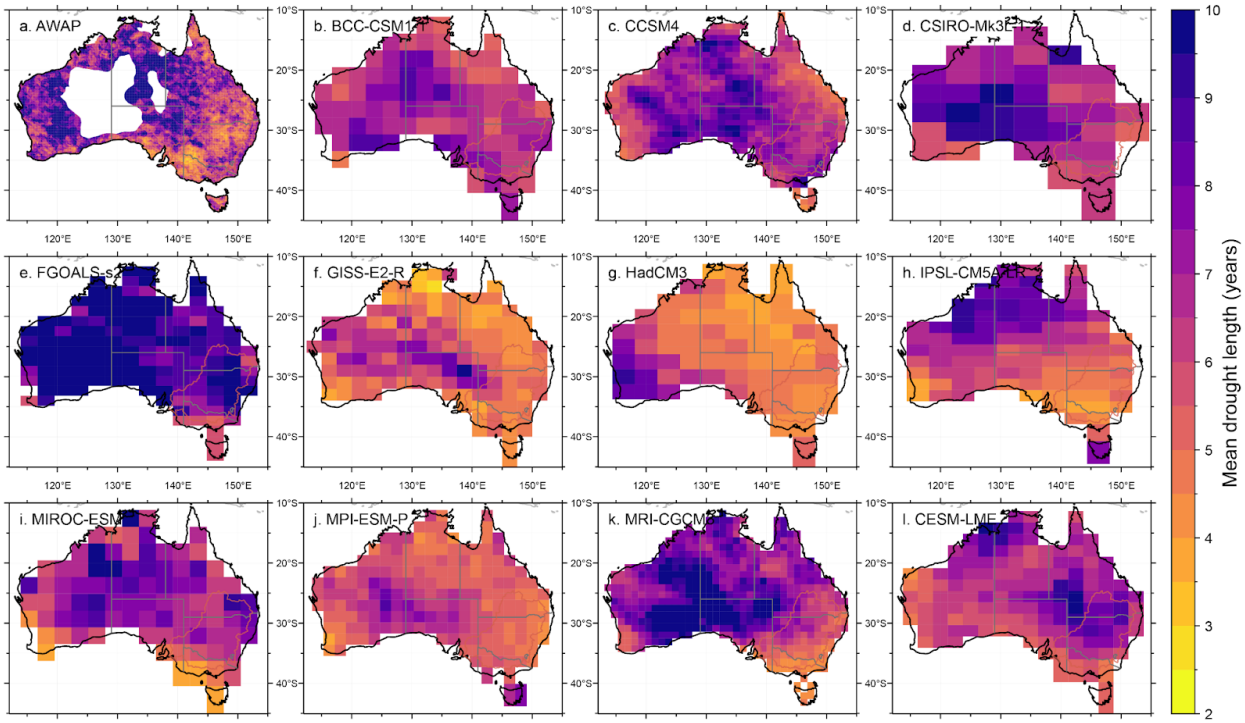

Figure S7: Mean multi-year drought length in (a) observations (1900–2000) and (b–l) model simulations of the pre-industrial last millennium (850-1849). Panel (l) shows the CESM-LME ensemble mean.

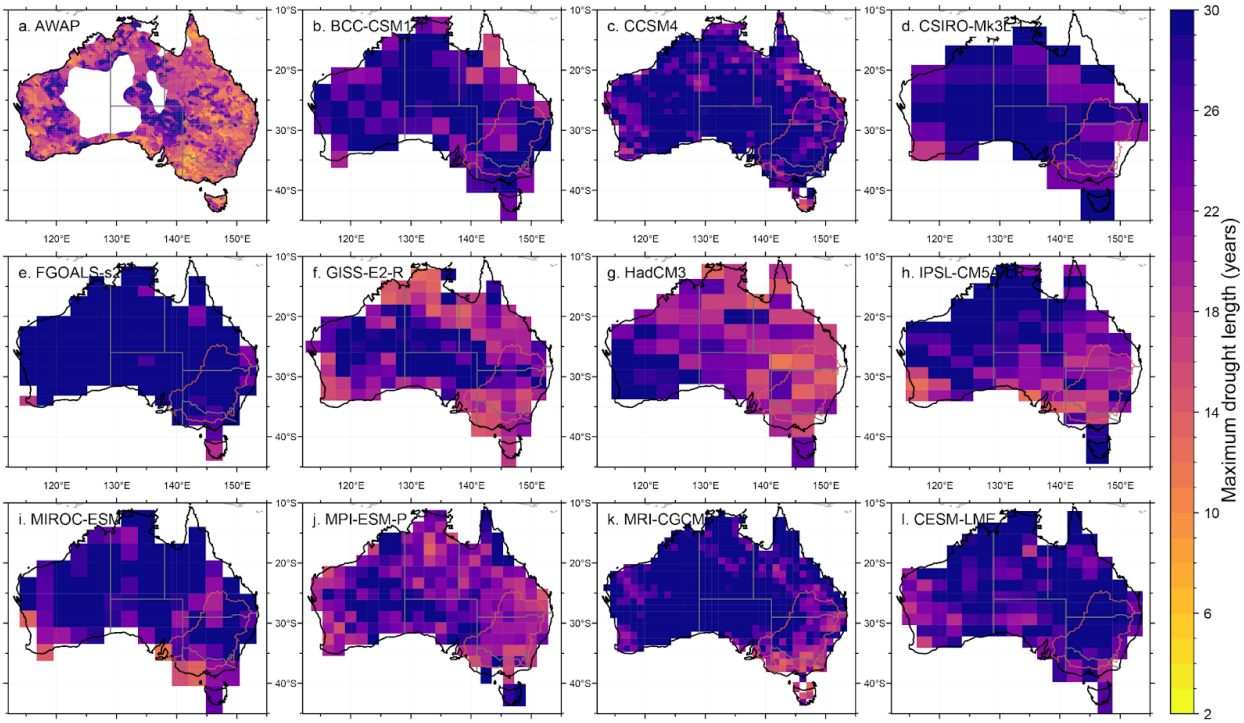

Figure S8: Maximum multi-year drought length in (a) observations (1900–2000) and (b–l) model simulations of the pre-industrial last millennium (850–1849). Panel (l) shows the CESM-LME ensemble mean.

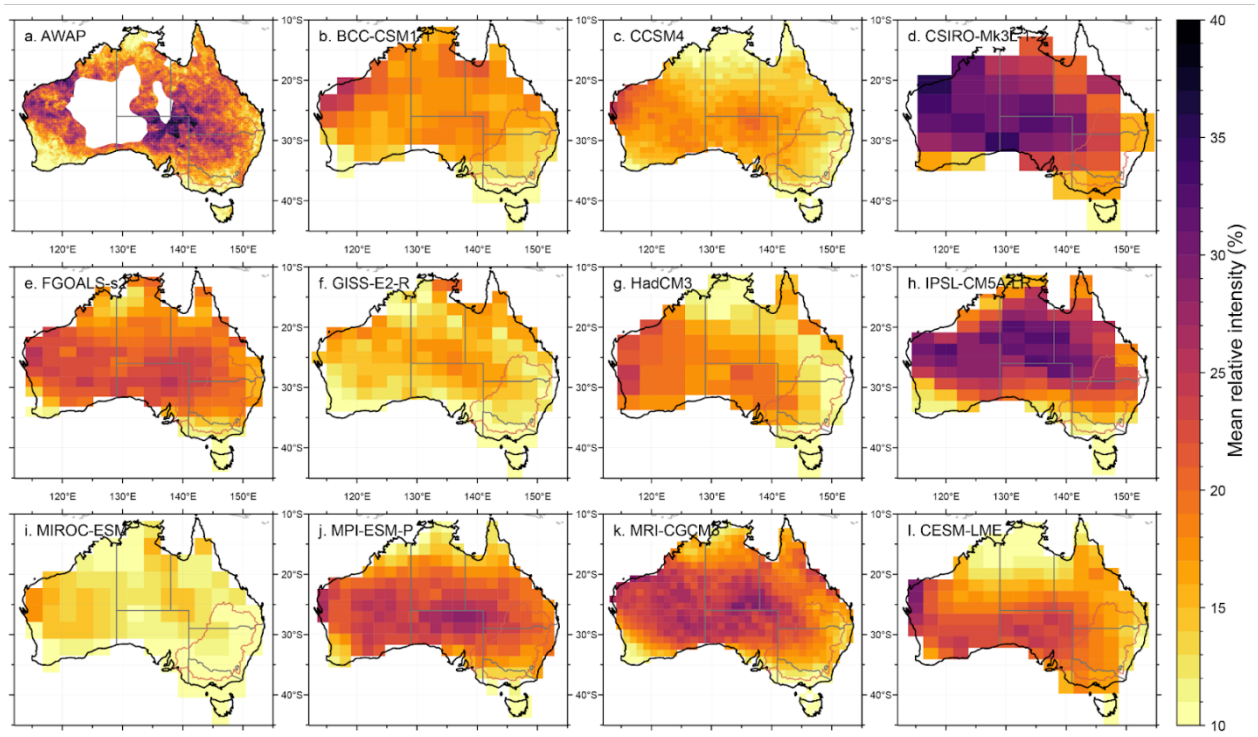

Figure S9: Relative intensity of multi-year droughts in (a) observations (1900–2000) and (b–l) model simulations of the pre-industrial last millennium (850–1849). Panel (l) shows the CESM-LME ensemble mean.

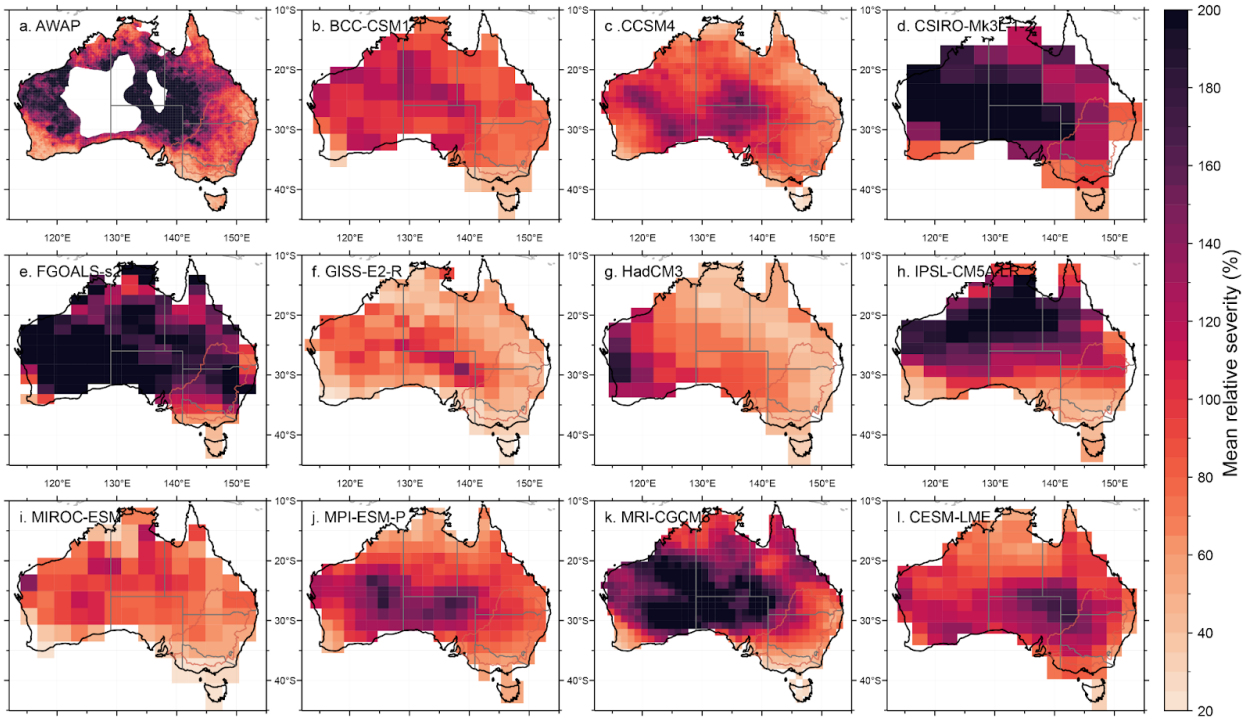

Figure S10: Relative severity of multi-year droughts in (a) observations (1900–2000) and (b–l) model simulations of the pre-industrial last millennium (850–1849). Panel (l) shows the CESM-LME ensemble mean.

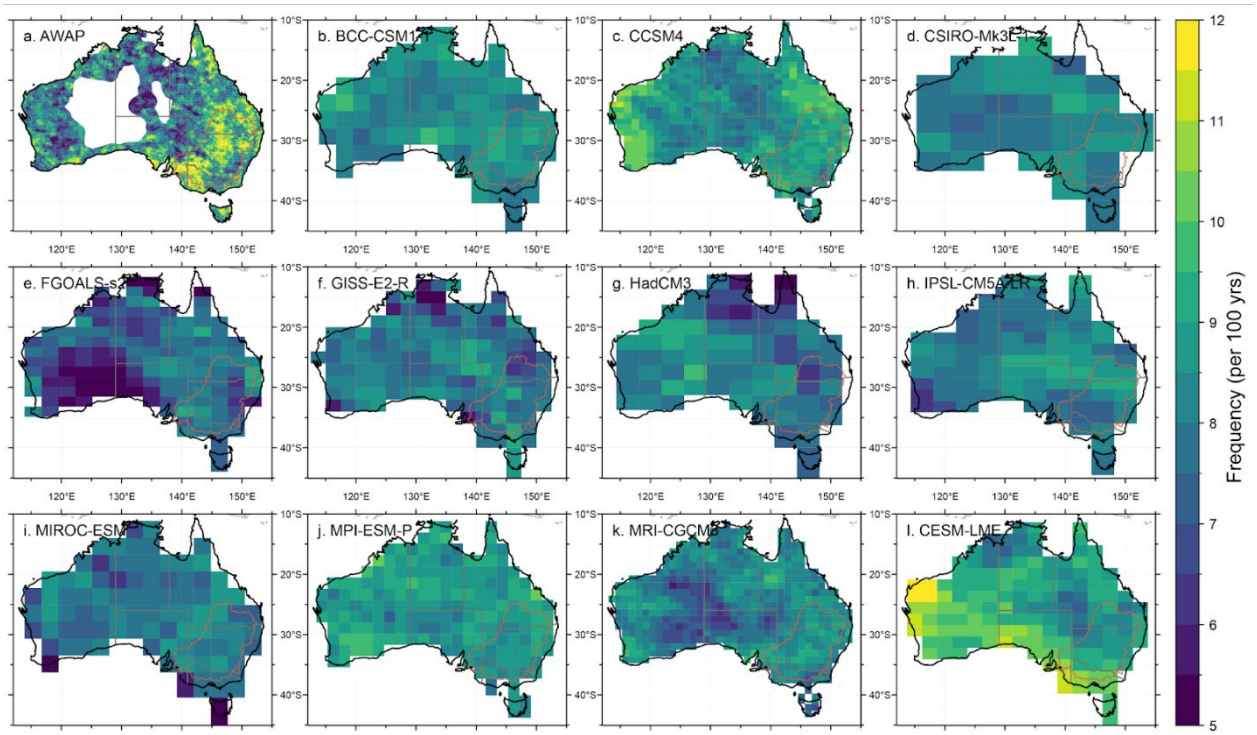

Figure S11: Frequency of multi-year droughts (per 100 years) in (a) observations (1900–2000) and (b–l) model simulations of the pre-industrial last millennium (850–1849). Panel (l) shows the CESM-LME ensemble mean.

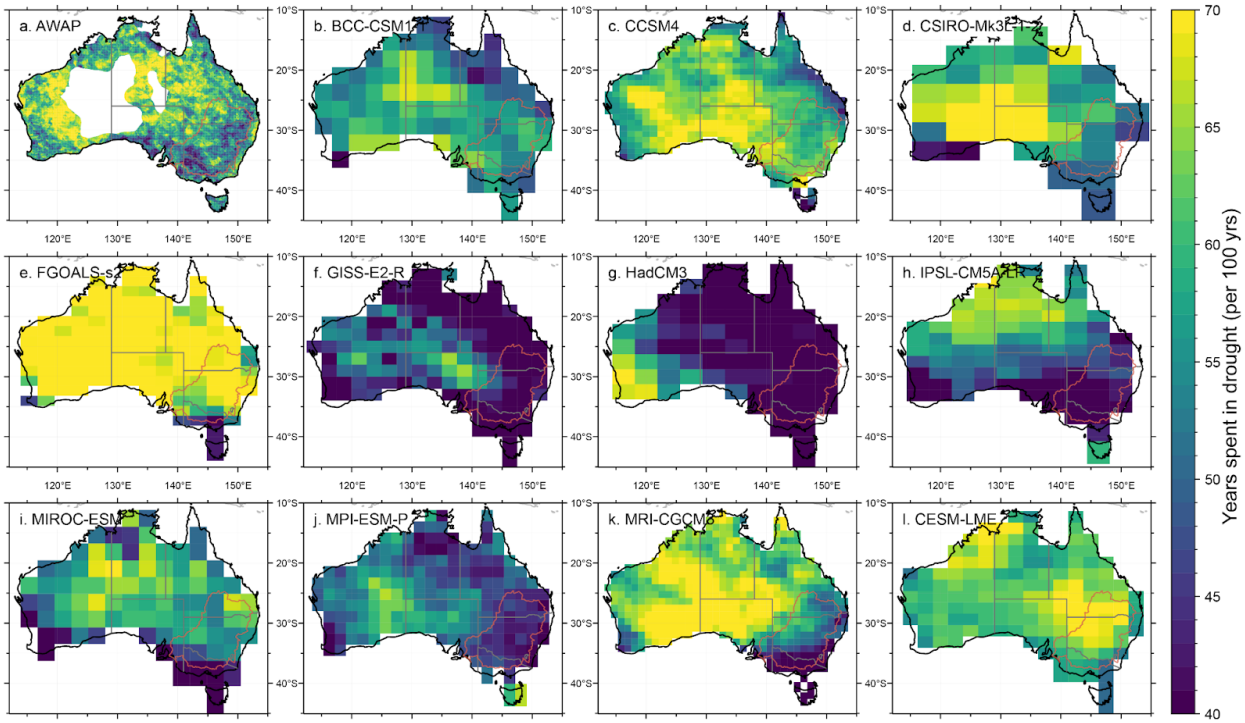

Figure S12: Total years spent in drought (per 100 years) in (a) observations (1900–2000) and (b–l) model simulations of the pre-industrial last millennium (850–1849). Panel (l) shows the CESM-LME ensemble mean.

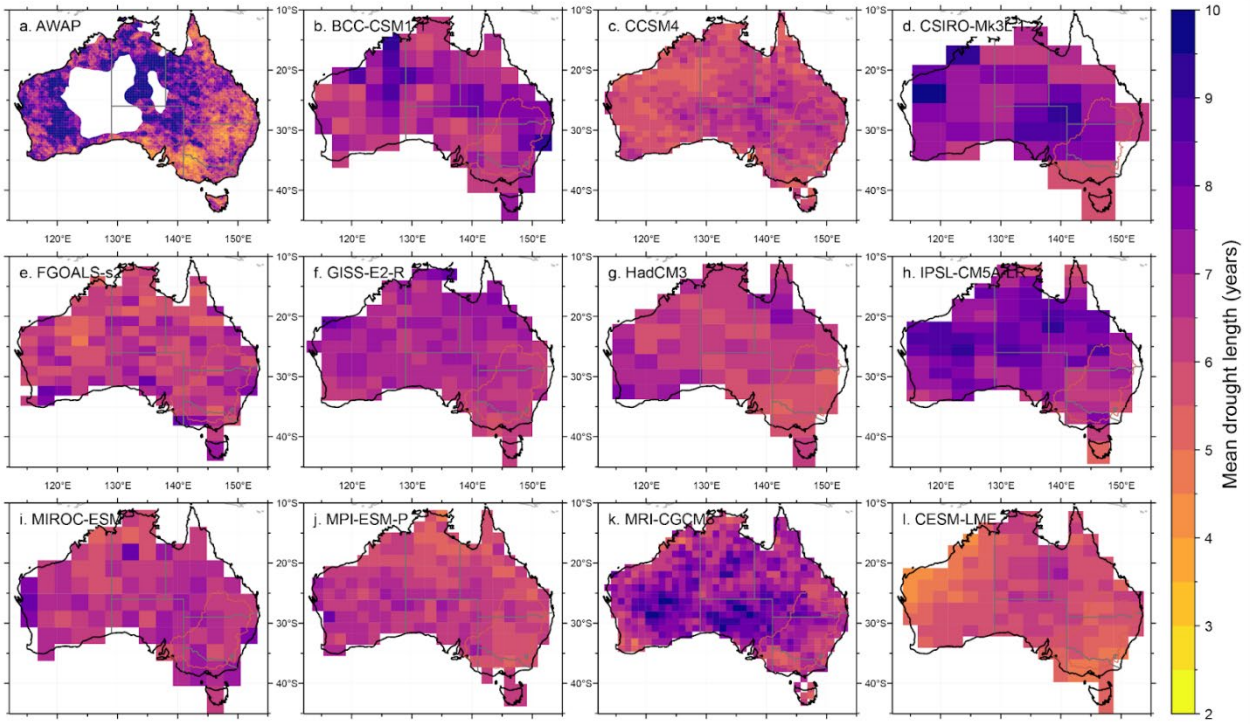

Figure S13: Mean multi-year drought length in (a) observations (1900–2000) and (b–l) piControl simulations.

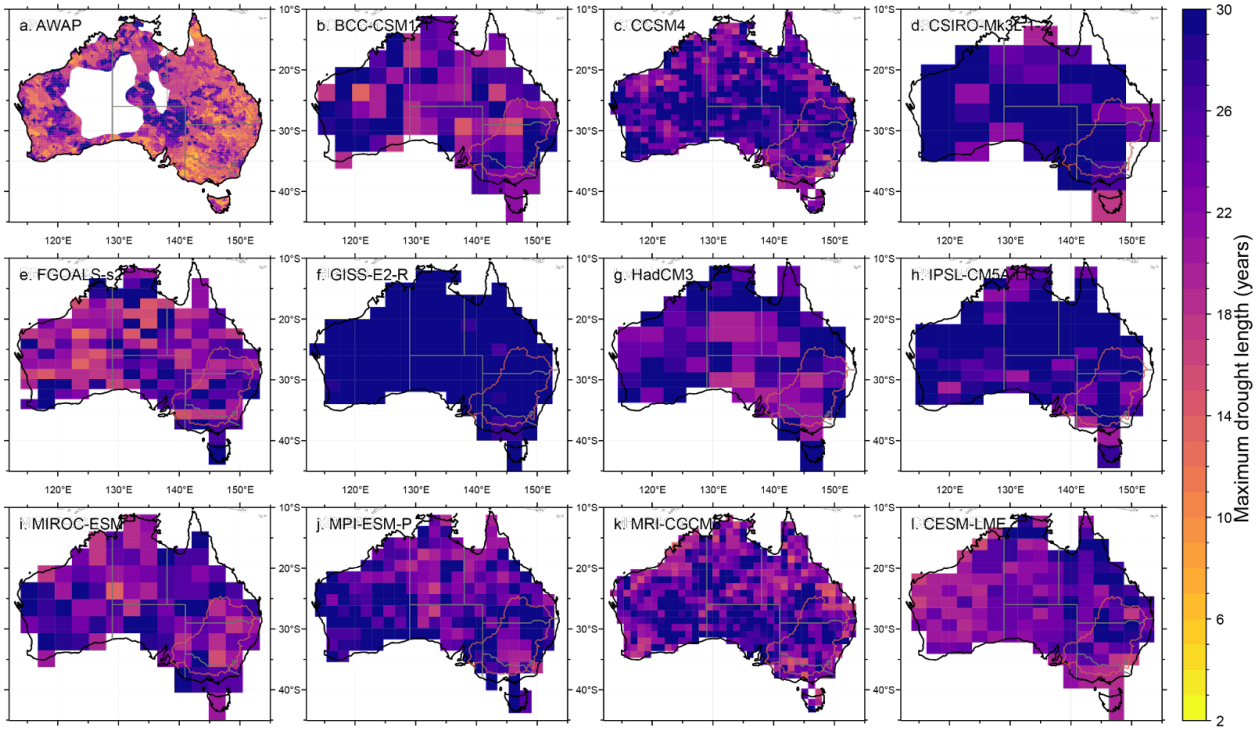

Figure S14: Maximum multi-year drought length in (a) observations (1900–2000) and (b–l) piControl simulations.

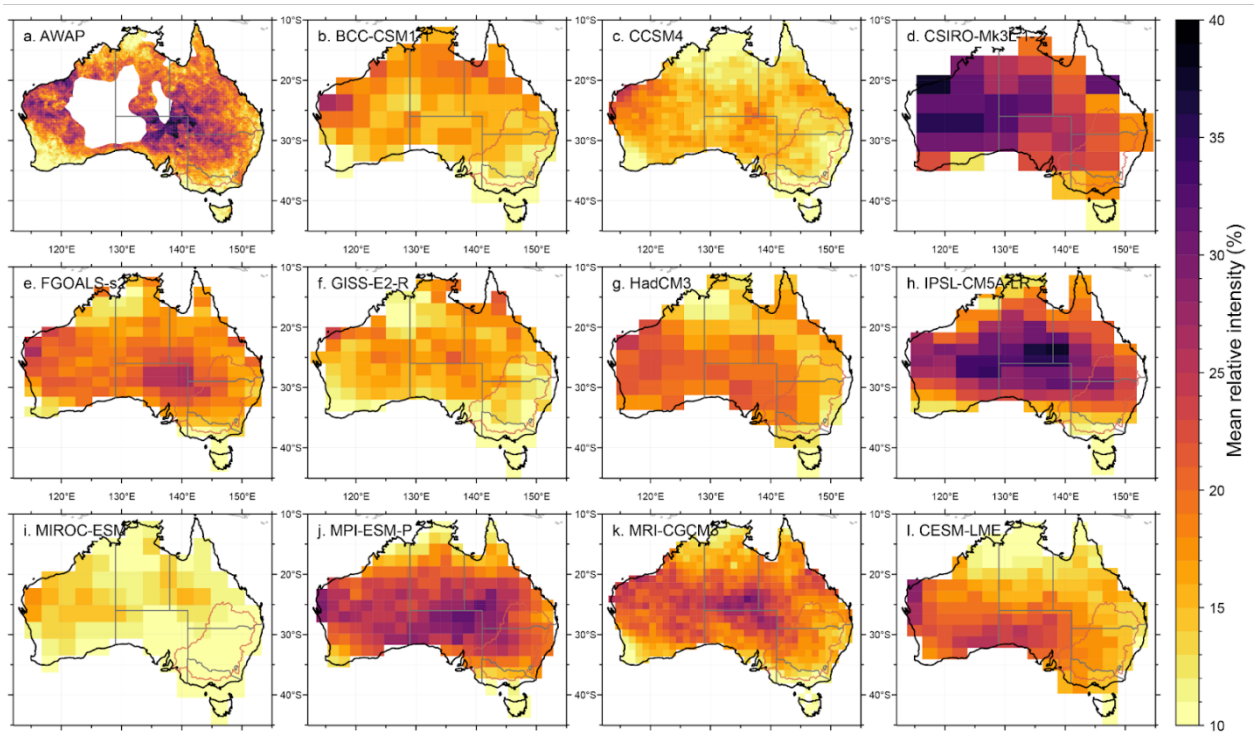

Figure S15: Relative intensity of multi-year droughts in (a) observations (1900–2000) and (b–l) piControl simulations.

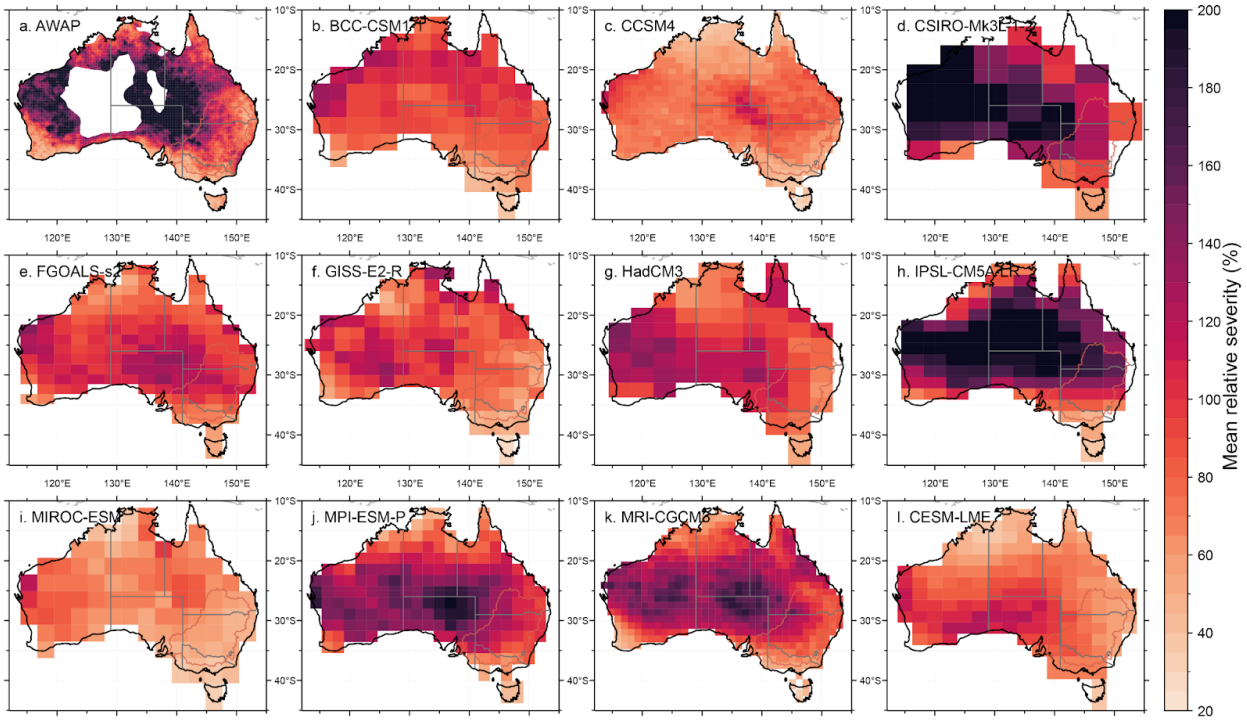

Figure S16: Relative severity of multi-year droughts in (a) observations (1900–2000) and (b–l) piControl simulations.

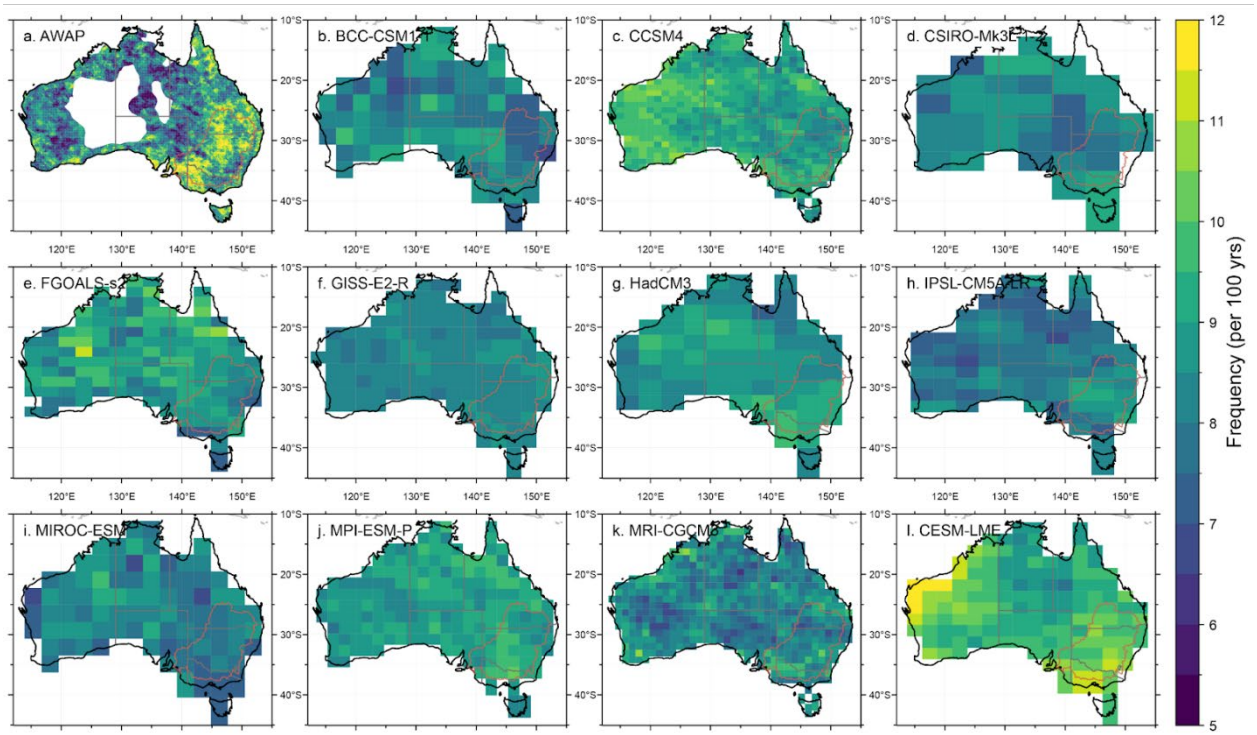

Figure S17: Frequency of multi-year droughts (per 100 years) in (a) observations (1900–2000) and (b–l) piControl simulations.

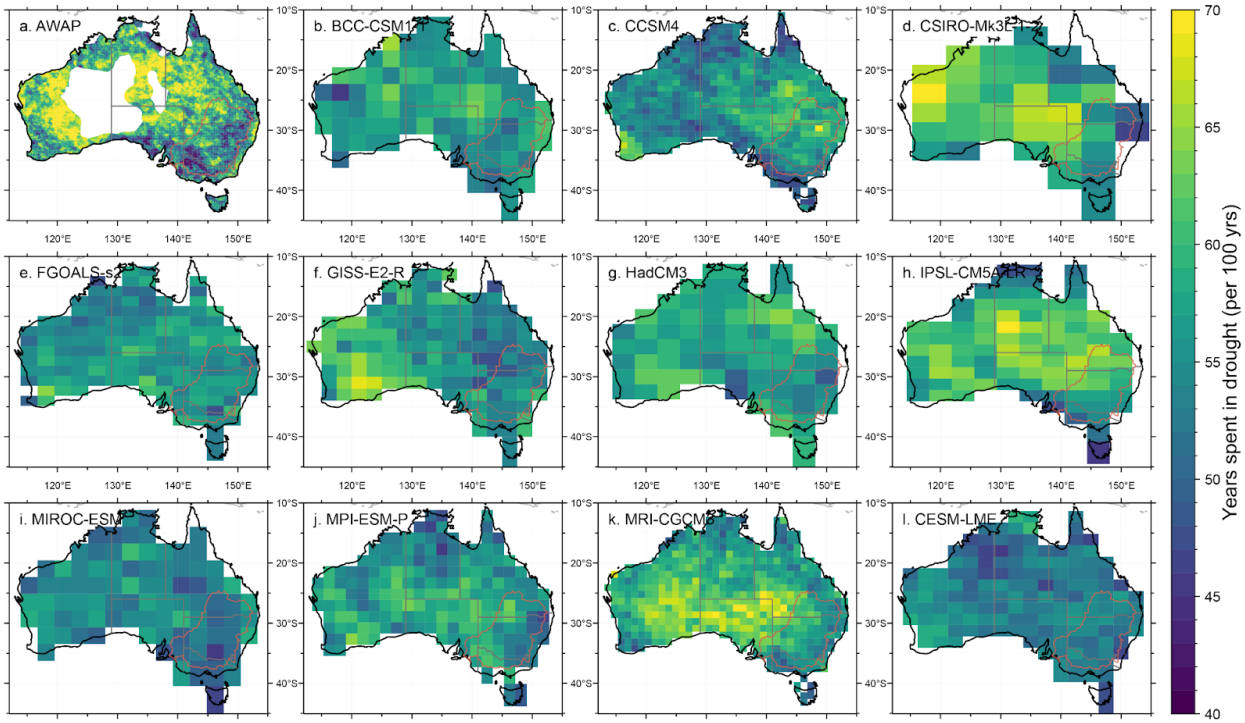

Figure S18: Total years spent in drought (per 100 years) in (a) observations (1900–2000) and (b–l) piControl simulations.

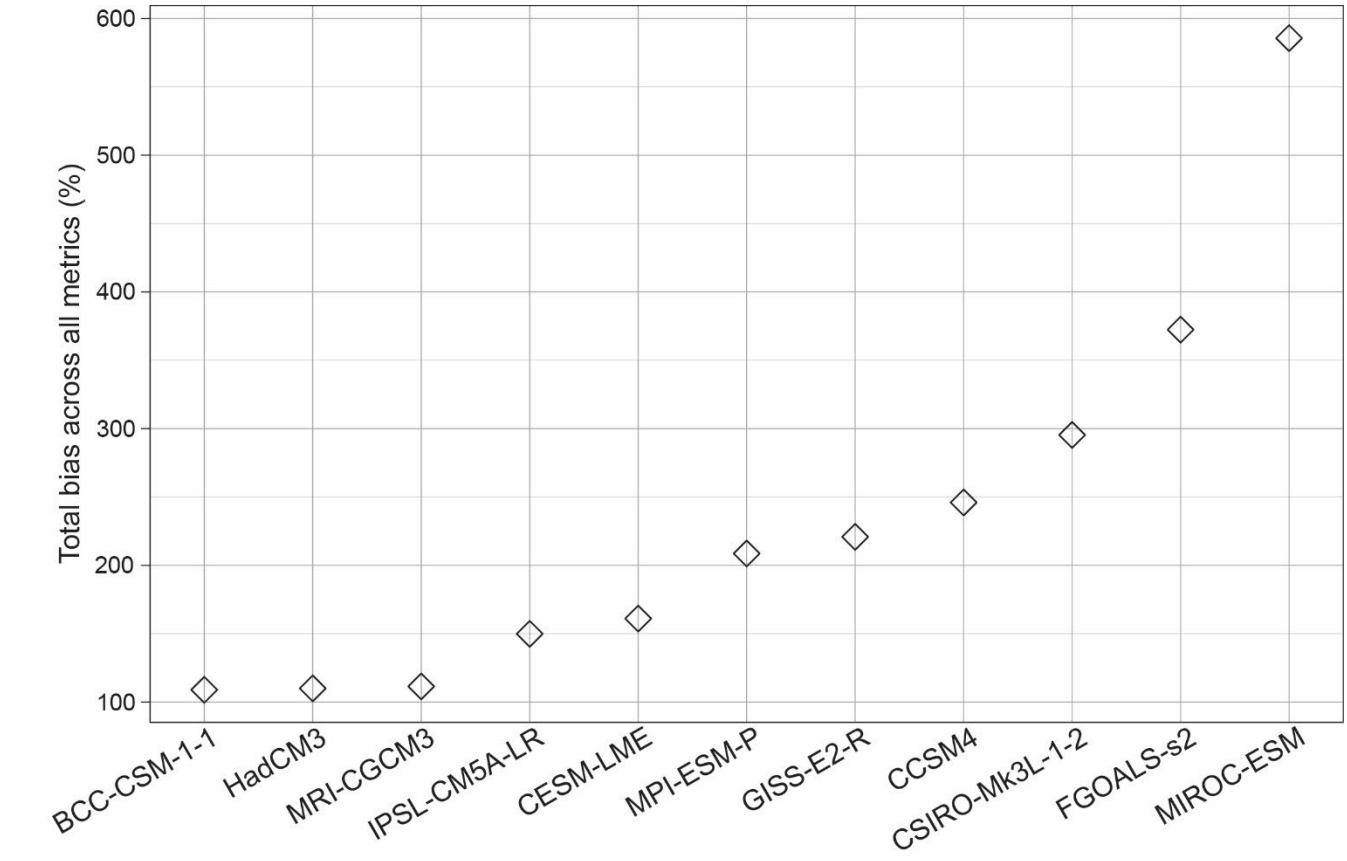

Figure S19. Summed percent bias for PMIP3/CMIP5 models and the CESM-LME, simulating drought metrics (CV, MAP, mean length, maximum length, intensity, severity, frequency, and proportion of time in drought) in the Murray-Darling Basin. Percent bias values for each model were calculated relative to the observed value in the twentieth century (1900–2000). Total bias was calculated using the absolute value for each metric. Showing the ensemble mean for the CESM-LME. Models are ordered from lowest to highest total bias along the x-axis; this ordering corresponds to the ordering of models in Fig. 6.

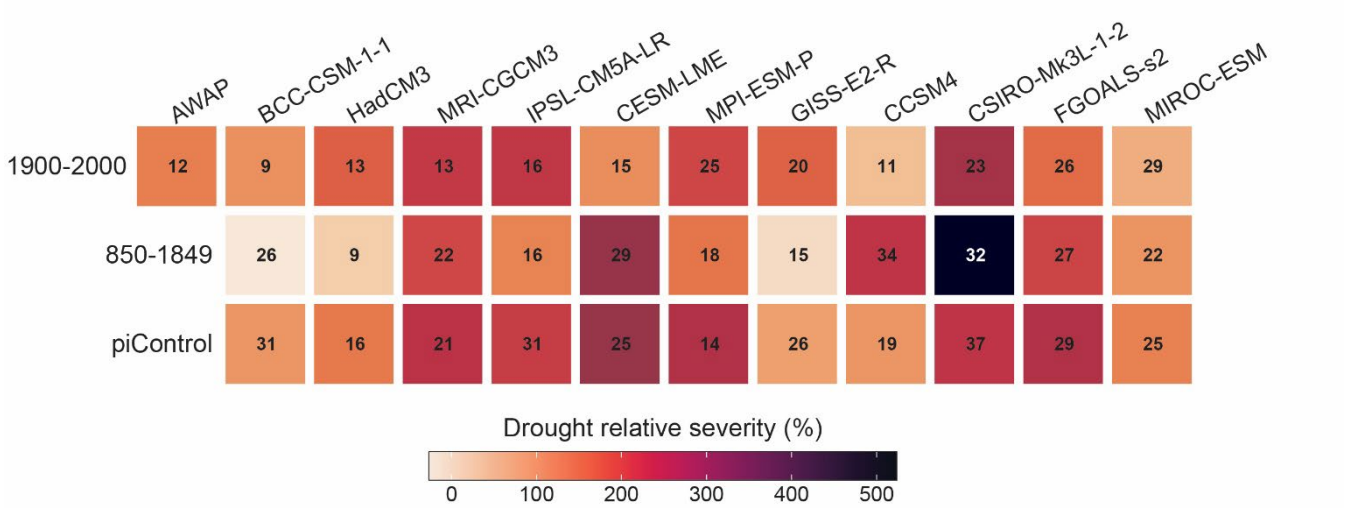

Figure S20. Relative severity of the single longest drought occurring in the Murray-Darling Basin in the HIST, piLM, and piControl simulations of each PMIP3/CMIP5 model, as well as observations. Tile colour corresponds to drought relative severity; that is, the cumulative deviation from climatological precipitation during the drought. Text on each tile states the total length of the drought (in years).

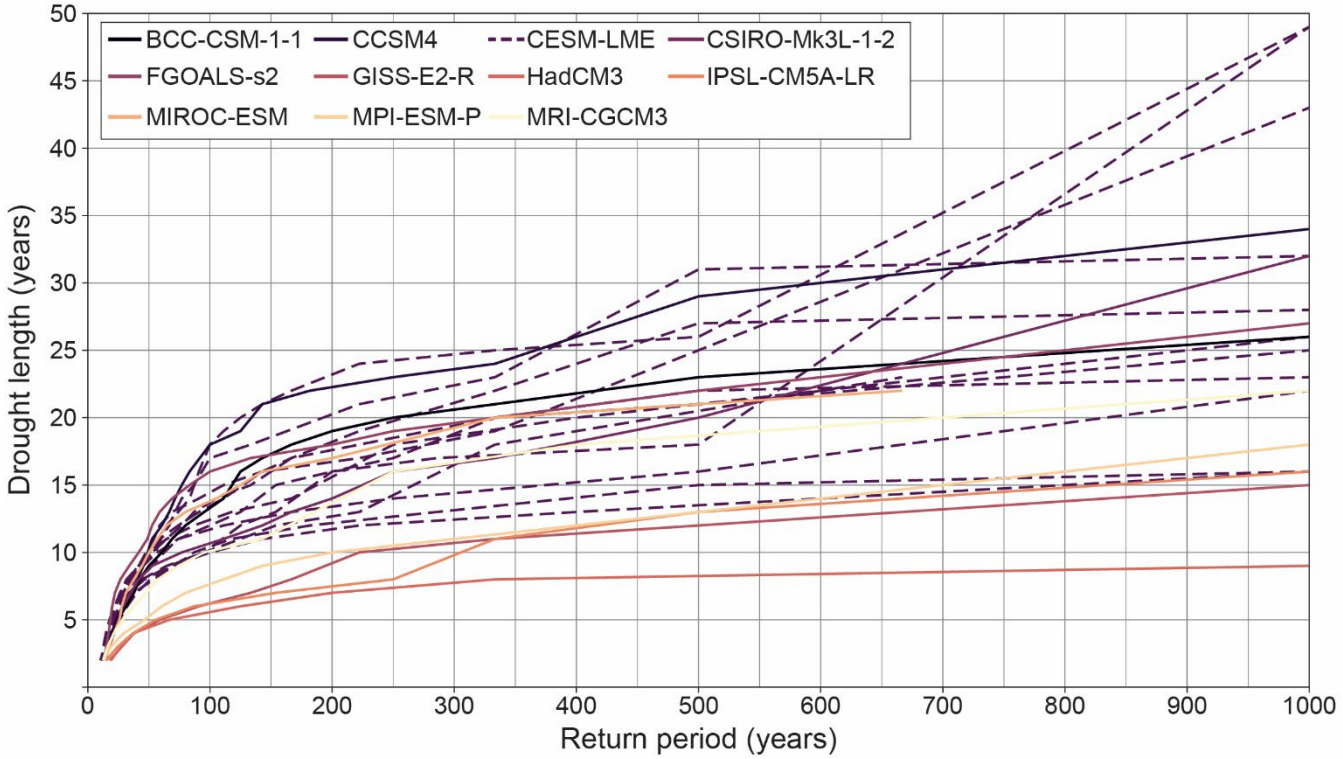

Figure S21. Return period of multi-year droughts in the Murray-Darling Basin, in the piLM simulations from each PMIP3/CMIP5 model (850-1849). Results from the single-model ensemble (CESM-LME, n = 13) shown in dashed lines.

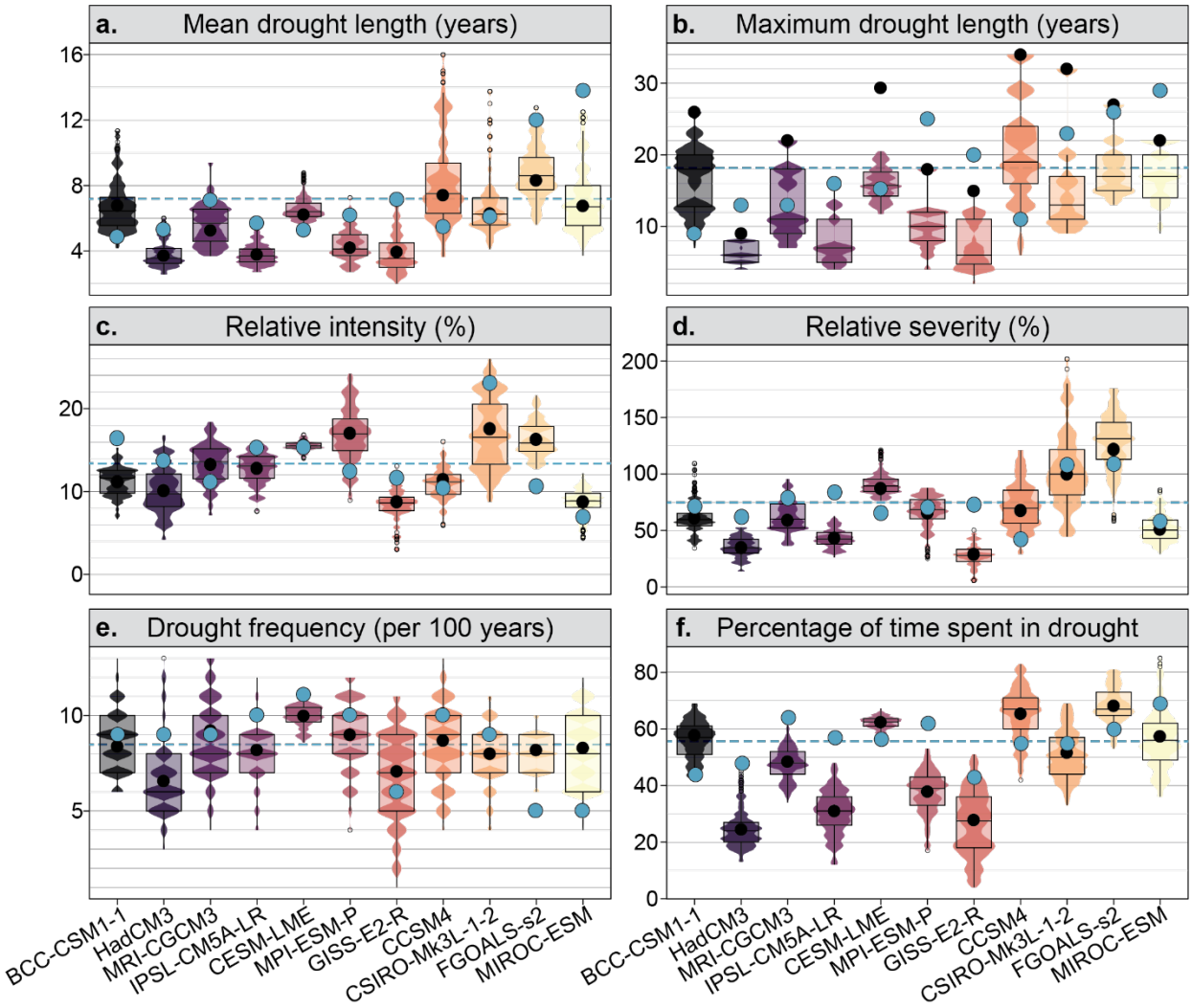

Figure S22. Comparison of Murray-Darling Basin drought metrics calculated on the HIST simulations from each model (1900–2000) versus many intervals of the same length subsampled from the longer piLM simulations. Violin-and-boxplots ('voxplots') show the distribution of values for each drought metric, for 500 randomly-sampled 101-year segments of the 1000-year-long piLM simulations, for each model. Black spots show the mean value for the *full* pre-industrial last millennium, for each model. Large blue spots show the value for 101-year HIST simulation, for each model. Dashed blue line shows the multi-model mean value for each metric in the HIST simulations. All panels show the CESM-LME ensemble mean. Models are ordered according to their summed percent bias across all drought metrics in the twentieth century (as per Fig. 8).

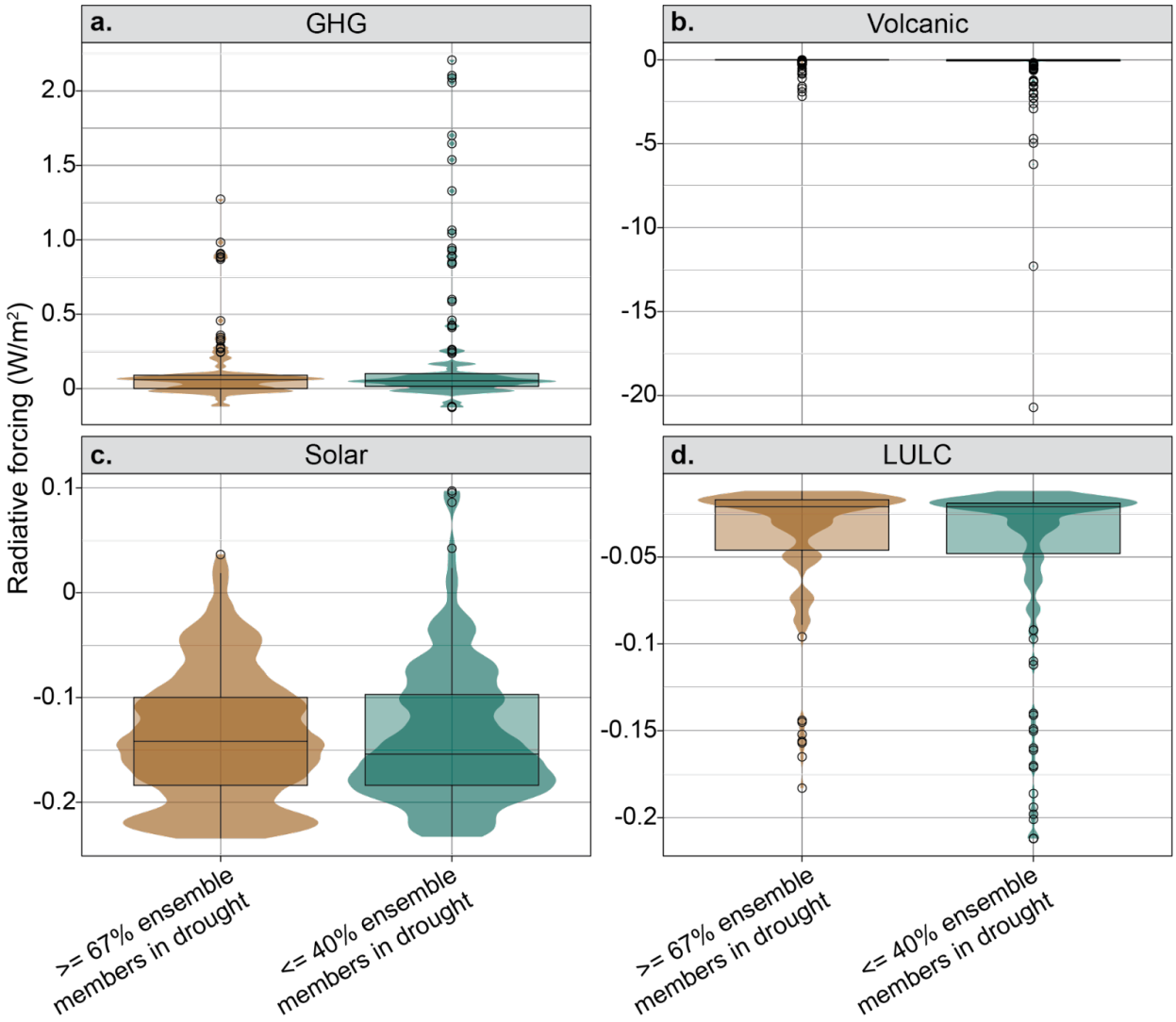

Figure S23. Magnitudes of external radiative forcings during periods where most ensemble members in the full CESM-LME (n=30) are in drought (brown voxplots) or not in drought (green voxplots). In the brown voxplots, at least 20 of the 30 ensemble members are in drought. In the green voxplots, 12 or fewer of the 30 ensemble members are in drought. This represents the upper and lower 10% of possible percentages of ensemble members in drought in any one year (i.e., colours in main text Fig. 10b). GHG = well-mixed greenhouse gases. LULC = land use and/or land cover changes.